RRKM and Ab Initio Investigation of the NH (X) Oxidation by Dioxygen

Marat R. Talipov,* Sergey L. Khursan, and Rustam L. Safiullin

Institute of Organic Chemistry, Ufa Scientific Centre, Russian Academy of Sciences, pr. Oktyabrya 71, Ufa, 450054 Russia

Received: March 20, 2009; Revised Manuscript Received: April 13, 2009

We performed a detailed study of the NH + O_2 potential energy surface by means of a number of multireference (CASSCF, MC-QDPT2, MR-AQCC, MR-CISD(18;13)+Q with 6-311+G(d,p), and *aug*-cc-pVTZ basis sets) and composite (G3B3, G3MP2B3, CBS-QB3, W1U) methods. Parent nitroso oxide, HNOO, was found to be the key intermediate of this process. In its ground state, $^1A'$, HNOO exists in two conformations, where the *cis* form is 8.1−10.9 kJ·mol^{-1} more stable than the *trans*-nitroso oxide. The mechanism of nitrene oxidation by dioxygen may be represented as a set of various transformations of vibrationally excited HNOO, namely, decomposition into NO and OH radical pair, O−O dissociation reaction, and a number of thermal deactivation processes. We localized all stationary points of these transformations on both the singlet and the triplet reaction PES. The energies of reactants, products, and transition states were calculated at the RI-MR-CISD(18;13)+Q/*aug*-cc-pVTZ level of theory; the vibrational analysis of these species was done by means of CASSCF(18;13)/6-311+G(d,p). Apparent rate constants of the NH + O_2 reaction were calculated using RRKM theory. The total rate constant k_{total} corresponds well to available experimental data. The temperature dependence of k_{total} is rather nontrivial and consists of three quasi-linear intervals. At low temperatures (up to room temperature) the slope of $\log(k_{total})$ vs $1/T$ is negative due to prevailing stabilization of HNOO. The rate-determining channel of the "NH + O_2" reaction in the medium-temperature interval (up to ∼1000 K) was found to be formation of the NO + OH radical pair via H transfer to the terminal oxygen atom. This reaction is accelerated by a factor of 4.2 (214 K) and 1.2 (2500 K) due to tunnel effect. The distinctive feature of the NH + O_2 high-temperature chemistry is the increase of the effective activation energy due to prevailing dissociation of the HNOO peroxide bond.

1. Introduction

Aromatic nitroso oxides (ArNOO) are key intermediates of aryl azides photooxidation.[1,2] The chemistry of these unique compounds has been analyzed in detail by Gritsan[3] and Sawwan.[4] Our interest in this area concerns the kinetics and mechanism study of the ArNOO self-reaction and its interaction with organic substances (for example, olefins).[5–10] At present the chemical behavior of nitroso oxides is not still clear. It was shown that the decay kinetics for some aromatic nitroso oxides (*para*-R-PhNOO, R = H−, Me−, NO_2−, Br−, Me_2N−, MeO−) obey the first-order law;[7,10] however, the reaction mechanism has no unequivocal proof. In particular, the question of formation of the nitroso compound, which is one of the major photo-oxidation products, is left open. The chemistry of nitroso oxides is complicated by evidence of the participation of triplet electronic states in the reactions of ArNOO.[11–14]

The lack of information on nitroso oxides is caused by the fact that these particles are difficult to access for both experimental and theoretical studies. Even the parent nitroso oxide HNOO is known to be the challenging object for theoretical modeling. The HNOO molecule as well as the parent carbonyl oxide H_2COO is isoelectronic with ozone. The most distinctive feature of its structure is known to be a three-center 4π-electron system, which is highly problematic to be correctly described even by sophisticated quantum-chemical methods.[15,16] In particular, it was shown[16] that optimization of HNOO geometric parameters leads to an error even at the QCISD(T) level of theory.

The reactions of HNOO represent another very important problem of nitroso oxide chemistry. It is known that reaction of nitrene NH ($^3\Sigma^-$) with molecular oxygen O_2 ($^3\Sigma_g^-$) proceeds via formation of nitroso oxide HNOO in the number of processes, namely, photooxidation of azides,[17] the reaction of ammonia with atomic fluorine,[18] and ammonia oxygen flames.[19] At moderate temperature (268−543 K) an activation barrier was determined in ref 18 to be equal to 6.4 ± 0.6 kJ·mol^{-1}. Analysis of experimental data[20–25] shows that in a wide temperature interval (270−3270 K) the NH + O_2 reaction rate constant may be expressed as a three-parameter function (eq 1), again with a low activation energy[26]

$$k(T) = A\left(\frac{T}{T_{ref}}\right)^n \cdot \exp\left(\frac{E_a}{RT}\right) \qquad (1)$$

where $A = 2.08 \times 10^{-14}$ cm^3/(molecule s), $n = 1.99$, $T_{ref} = 298$ K, $E_a = 2.06$ kJ·mol^{-1}, and rmsd = 0.16.

It was found[19] that NO and OH are the main products at low-temperature conditions (<573 K). According to ref 20, an effective activation energy of this reaction is 5.0 kJ·mol^{-1}. There are two hypotheses of the mechanism of NO and OH formation from HNOO: either via intermediate formation of dioxaziridine[19] (Figure 1a) or via direct isomerization of nitroso oxide[27] (Figure 1b). At present, there is not clarity regarding this question.

At higher temperatures the major products of HNOO transformation became HNO and atomic oxygen. An activation

* To whom correspondence should be addressed. E-mail: TalipovMR@anrb.ru.

10.1021/jp902527a CCC: $40.75
Published on Web 05/14/2009

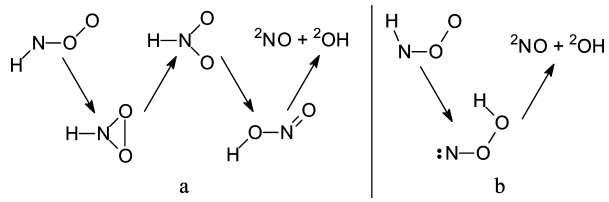

Figure 1. Possible pathways of the NO + OH radical pair formation.

energy for this reaction pattern is substantially higher, 74.8 kJ·mol^{-1}.[22] HNO + O formation was believed to proceed via the O−O bond breaking of triplet nitroso oxide.[28] However, it should be noted that singlet nitroso oxide can also dissociate to form triplet nitroso compound.

Our present work is devoted to solving of above-mentioned problems. It is clear that reactions of nitroso oxides carried out with substances with an unusual electronic nature may be correctly described only by intensively accounting for both the dynamic and static correlation energy. That is the reason for applying multireference methods of quantum chemistry to modeling of the process of formation and decomposition of the parent nitroso oxide. In our opinion, this process is both significant itself and a good model to understanding the chemical behavior of higher analogs of HNOO, aromatic nitroso oxides.

2. Computational Methods

Calculation of the geometry of nitroso oxide, in particular, the N−O and O−O distances, is known to be challenging for computational chemistry[16,29] in spite of the necessity for intensively accounting for both static and dynamic electron correlation. The problem can be solved correctly at least at the CCSD(T) or CASSCF level of theory (Table 1). The anharmonic vibration frequencies of *trans*-HNOO calculated in ref 16 by means of the CCSDT-3(Q_f)/cc-pVTZ level of theory (650, 757, 1071, 1126, 1499, 3188 cm^{-1}) are in good agreement with experimental data (−, 764.0, 1054.5, 1092.3, 1485.5, 3165.5 cm^{-1} [17]). Despite the harmonic approximation, the CASSCF(18;13)/6-311+G(d,p) frequencies are close to the experimental results (658.5, 766.8, 1043.9, 1118.1, 1539.8, 3253.5 cm^{-1}, without a scale factor). In accordance, geometry and vibration spectra of HNO_2 isomers were also calculated at the CASSCF(18;13)/6-311+G(d,p) level of theory. The decomposition products (NH + O_2, HNO + O, NO + OH) were separately optimized at the same level of theory with full valence active spaces resulting in the same (18;13) total active space for each pair. Sophisticated multireference MC-QDPT2, MRCI, and MR-AQCC calculations as well as a number of composite procedures G3,[30] G3MP2B3,[31] CBS-QB3,[32] and W1U[33] were used for precise molecular energy computations.

Quantum-chemical calculations were carried out using PC Gamess v7.1[34,35] and Orca 2.0 packages.[36]

The NH + O_2 recombination is known to be a highly exothermic reaction. Under gas-phase conditions the particles distribution function can considerably differ from the Boltzmann distribution. In the falloff or low-pressure limit the slow energy exchange with a bath gas increases the role of vibrationally excited states. Chemically activated nitroso oxide possesses sufficient additional energy to overcome the barrier of the reverse dissociation or another unimolecular reaction. This aspect cannot be accounted for by the Eyring equation because it is applicable only in the high-pressure limit regime; so, we applied the Rice−Ramsperger−Kassel−Markus theory (RRKM) to calculate the basic reaction values, a set of microscopic rate constants κ_i, for kinetic analysis of Scheme 1.

To calculate the apparent rate constants k_1-k_8 (Scheme 1, k_1-k_4 are the rate constants of the accumulation of corresponding products; k_5-k_8 are the rate constants of the thermal deactivation of chemically activated molecules) we applied the method proposed in ref 37, which combines chemical activation distribution functions and QRRK methods to predict the kinetics of gas-phase reactions. This approach was approbated[19,38] on systems similar to ours. The steady-state approximation for the concentration of vibrationally excited HNOO was used eqs 2 and 3

$$k_{1-4} = \frac{1}{[\mathrm{NH}][\mathrm{O_2}]} \sum_{i}^{\text{all processes}} \int_0^\infty k_i(E) C^*(E)\, \mathrm{d}E \qquad (2)$$

$$k_{5-8} = \frac{1}{[\mathrm{NH}][\mathrm{iO_2}]} \int_0^\infty \omega C^*(E)\, \mathrm{d}E \qquad (3)$$

where $\kappa_i(E)$ is the microscopic rate constant (see eq 4), ω is the rate of thermal deactivation of the vibronically excited molecules (see eq 5), $C^*(E)$ is the steady-state concentration of the microcanonical ensemble of HNOO in different electronic states (singlet or triplet) in different configurations (*cis* or *trans*).

$$k_i(E) = \frac{Q_r^{\ddagger}}{Q_r} \frac{W^{\ddagger}(E - E_{\min})}{hN(E)} \qquad (4)$$

In the latter equation $Q_r^{\ddagger}$, Q_r are the rotational partition functions of the activated complex and reactant. The number of vibrational levels of the transition state $W^{\ddagger}(E - E_{\min})$ and the density of reactants' vibrational levels $N(E)$ were calculated according to the Witten and Rabinovich approximations (eqs SI.9−SI.14, Supporting Information).

The rate constant of thermal deactivation of the vibronically excited molecules was calculated according to refs 39 and 40 by eq 5

$$\omega = \beta_c Z_{\mathrm{LJ}} \Omega^{*(2.2)} \qquad (5)$$

where Z is the Lennard−Jones collision frequency (eq SI.15, Supporting Information) in the variation proposed by Robinson,[39] β_c is the collision efficiency (eq SI.16, Supporting Information), and $\Omega^{*(2.2)}$ is the correction for the elastic collisions (eq SI.17, Supporting Information).

The proton transfer reaction is known to be complicated with a tunnel effect. The tunneling probability was estimated by replacing $W^{\ddagger}(E - E_{\min})$ in eq 4 with $W_{\text{tunnel}}(E)$

$$W_{\text{tunnel}} = \int_0^{E+V_0} N(x) P(E - x)\, \mathrm{d}x \qquad (6)$$

where $P(E)$ is the one-dimensional tunneling probability calculated using the generalized Eckart potential (see eqs SI.18−SI.21, Supporting Information).[41]

Expressions 7−10 for the steady-state concentrations of the microcanonical ensemble of *cis*-^{1}HNOO*, *trans*-^{1}HNOO*, *cis*-^{3}HNOO*, and *trans*-^{3}HNOO* (further designated as $C^*_{1c}(E)$,$C^*_{1t}(E)$, $C^*_{3c}(E)$, and $C^*_{3t}(E)$ were obtained from Scheme 1

$$C^*_{1c}(E) = \frac{k_3 f_{1c}(E) A_{1t}(E) + k_{-1}(E) k_4 f_{1t}(E)}{A_{1t}(E) A_{1c}(E) - k_{-1}(E) k_1(E)} \qquad (7)$$

$$C^*_{1t}(E) = \frac{k_4 f_{1t}(E) A_{1c}(E) + k_1(E) k_3 f_{1c}(E)}{A_{1t}(E) A_{1c}(E) - k_{-1}(E) k_1(E)} \qquad (8)$$

TABLE 1: Geometrical Parameters of HNOO

	UB3LYP/ 6-31G(d)	MCSCF(6;6)/ 6-31G(d,p)[27]	CCSD(T)/ 6-311G(d,p)[17]	CCSD(T)/ cc-pVTZ[16]	CR-CCSD(T)/ cc-pVT[16]	CCSDT-3(Qf)/ cc-pVTZ[16]	CASSCF (18;13)/ 6-311+G(d,p)	MR-AQCC(8;7)/ cc-pVTZ
cis								
R(OO), Å	1.310	1.253	1.306				1.312	1.318
R(NO), Å	1.286	1.295	1.290				1.296	1.288
R(NH), Å	1.040	1.031	1.040				1.049	1.034
A(NOO), deg	119.0	119.0	118.8				118.5	119.0
A(HNO), deg	103.9	104.8	103.5				103.8	103.9
trans								
R(OO), Å	1.299	1.251	1.293	1.295	1.281	1.286	1.297	1.297
R(NO), Å	1.311	1.306	1.306	1.299	1.288	1.306	1.317	1.309
R(NH), Å	1.035	1.027	1.032	1.029	1.027	1.020	1.041	1.026
A(NOO), deg	115.3	115.9	116.0	115.9	116.5	116.0	116.1	115.8
A(HNO), deg	100.0	100.5	99.4	99.8	100.1	99.5	99.6	99.6

SCHEME 1

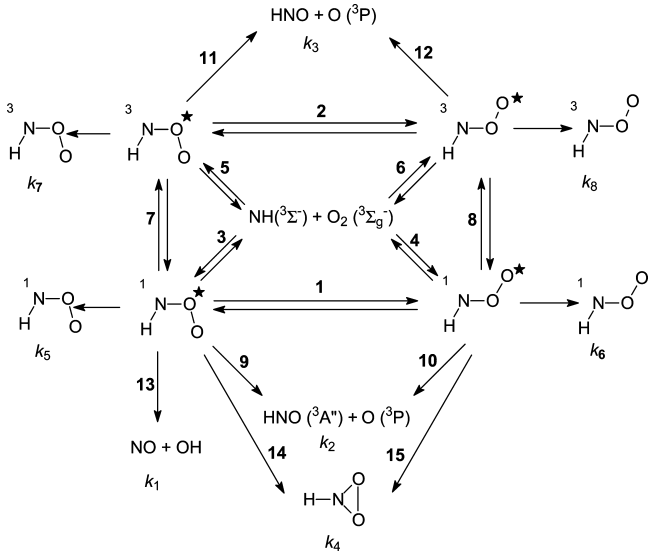

$$C^{*}_{3c}(E) = \frac{k_5 f_{3c}(E) A_{3t}(E) + k_{-2}(E) k_6 f_{3t}(E)}{A_{3t}(E) A_{3c}(E) - k_{-2}(E) k_2(E)} \quad (9)$$

$$C^{*}_{3t}(E) = \frac{k_6 f_{3t}(E) A_{3c}(E) + k_2(E) k_5 f_{3c}(E)}{A_{3t}(E) A_{3c}(E) - k_{-2}(E) k_2(E)} \quad (10)$$

where A is the microscopic constant for consumption of the corresponding particle, eqs 11−14

$$A_{1c}(E) = \omega + k_{-3}(E) + k_1(E) + k_9(E) + k_{14}(E) + k_{13}(E) \quad (11)$$

$$A_{1t}(E) = \omega + k_{-4}(E) + k_{-1}(E) + k_{10}(E) + k_{15}(E) \quad (12)$$

$$A_{3c}(E) = \omega + k_{-5}(E) + k_2(E) + k_{11}(E) \quad (13)$$

$$A_{3t}(E) = \omega + k_{-6}(E) + k_{-2}(E) + k_{12}(E) \quad (14)$$

The steady-state concentrations of HNOO* depend on the distribution of the chemically activated molecules on the energies $f(E)$, which was estimated by eq 15,[39] and the denominator was calculated numerically.

$$f(E) = \frac{W^{\ddagger}(E - E_{\min}) e^{-E/k_B T}}{\int_{E_{\min}}^{\infty} W^{\ddagger}(E_i - E_{\min}) e^{-E_i/k_B T} \, dE_i} \quad (15)$$

3. Results

Stable HNOO Forms. It is obvious that there are two possibilities in the N-substituent orientation; it explains the existence of quasi-degenerate *cis*- and *trans*-conformations of singlet RNOO. Our results obtained by sophisticated methods undoubtedly testify to the superior stability of *cis*-^{1}HNOO over the *trans* form by 8.1−10.9 kJ·mol^{-1} (Table 2). The conformational transition state (TS) separates the isomeric forms of HNOO with the rather high potential barrier of 119.4 kJ·mol^{-1} (Figure 2a), which hinders their interconversion at low temperatures.

The scan of the ^{3}HNOO potential energy surface (PES) at the CASSCF(18;13)/6-311+G(d,p) level of theory also revealed two conformations of nitroso oxide. In a similar manner with singlet HNOO, HN−OO dihedral angles correspond to planar forms of the molecule. It is curious that the number of approximations (the B3LYP hybrid potential with 6-31G(d), CBS-B7, cc-pVTZ+d, and 6-311+G(d,p) basis sets; the MC-QDPT2//CASSCF(18;13)/6-311+G(d,p) level of theory) show that the minima on the triplet PES correspond to the dihedral angles D(HN−OO) ∼30° and 180.0° (Figure SI.1, Supporting Information). Nevertheless, intensive account of both the static and dynamic electron correlation at the RI-MR-CISD(18;13)+Q/*aug*-cc-pVTZ level of theory has clarified that the *cis* form is more stable than the *gauche* form by 11.6 kJ·mol^{-1}. We localized the *cis*/*trans*-transition state (Figure 2b), the activation barrier to the *trans* form being 12.0 kJ·mol^{-1}, showing free interconversion of conformers.

Homolytic Cleavage of the N−O Bond. Choosing the N−O bond as a reaction coordinate for PES scanning we investigated the formation of singlet nitroso oxide from nitrene and molecular oxygen (Figure 3a) at the MC-QDPT2(18;13)//CASSCF(18;13)/6-311+G(d,p) level of theory. We found maxima on this PES which correspond to the transition states of reactions 3 and 4. The nature of the TSs was confirmed by their subsequent full optimization and Hessian computation. It is noteworthy that the transition state for the NH + O_2 reaction was not localized before despite clear experimental evidence of the activation nature of this reaction (see Introduction). Another interesting feature of this reaction is that the *trans*-oriented TS has become slightly more stable than the *cis*-TS despite the greater stability of *cis*-^{1}HNOO. The N−O (O−O) bond lengths in transition states were found to be 1.901 (1.230) and 1.895 (1.226) Å for the *cis* and *trans* forms, respectively. According to the Hammond postulate,[42] the large N−O interatomic distance as well as slight elongation of the O−O bond witnesses too the "early" nature of the TS.

The triplet PES of HNOO along the N−O coordinate also has one minimum and one maximum for both *cis*- and *trans*-HNOO. The former corresponds to the triplet nitroso oxide and the latter to the transition state of its formation (reactions 5 and 6). We successfully reoptimized all stationary points of the PES.

TABLE 2: Activation and Reaction Enthalpies for the HN + O_2 System (at 298 K, kJ·mol^{-1})

	MCQDPT2/BS1[a]		MR-AQCC/BS1		MR-CISD(18;13)+Q/BS1		RI-MR-CISD(18;13)+Q/BS2		G3MP2B3		G3		CBS-QB3		W1U	
eq	$\Delta H^{\ddagger}$	ΔH_r	$\Delta H^{\ddagger}$	ΔH_r	$\Delta H^{\ddagger}$	ΔH_r	$\Delta H^{\ddagger}$	ΔH_r	$\Delta H^{\ddagger}$	ΔH_r	$\Delta H^{\ddagger}$	ΔH_r	$\Delta H^{\ddagger}$	ΔH_r	$\Delta H^{\ddagger}$	ΔH_r
1	115.1	8.1	112.6	10.4	115.8	9.0	119.4	9.5		10.9		10.8		10.9		10.8
2	1.0	0.4	12.5	0.8	11.7	0.1	12.0	1.8	6.3	2.4	6.2	2.7	5.9	3.2		3.1
3	9.6	−71.9	9.2	−79.2	6.0	−87.4	−9.4	−108.5		−116.5		−117.8		−130.2		−122.5
4	5.7	−63.7	5.7	−68.8	3.4	−78.4	−11.8	−98.9		−105.6		−107.0		−119.3		−111.8
5	44.8	35.9	44.6	32.2	38.0	22.3	18.4	7.4		0.0		−0.4		−10.6		−6.0
6	42.6	36.4	42.2	33.1	36.2	22.4	18.2	9.3		2.4		2.3		−7.4		−2.9
7		107.8		111.5		109.8		115.9		116.6		117.4		119.6		116.6
8		100.1		101.9		100.9		108.2		108.0		109.3		111.9		108.9
9		149.1		151.6		155.3		175.0		196.6		197.4		201.6		195.0
10		140.9		141.2		146.3		165.5		185.6		186.6		190.6		184.3
11	25.2	−10.4	27.9	−30.3	30.3	−27.6	29.6	−12.5	53.1	3.3	52.3	4.0	48.5	4.6	56.4	2.6
12	40.6	−10.9	42.7	−31.1	46.2	−27.7	44.9	−14.3	68.2	0.9	67.1	1.3	64.7	1.3	70.6	−0.5
13	120.8	−111.5	119.4	−122.8	119.1	−122.4	118.4	−109.2	113.3	−111.1	113.8	−108.0	116.1	−103.8	112.5	−107.8
14	152.4	60.7	162.1	54.9	159.1	50.3	156.6	35.4		38.6		39.0	138.3	32.0	145.5	33.7
15	154.6	52.6	162.2	44.4	160.3	41.3	159.9	25.9		27.6		28.2	139.6	21.0	147.2	22.9

[a] BS1 denotes 6-311+G(d,p) basis set; BS2 denotes *aug*-cc-pVTZ.

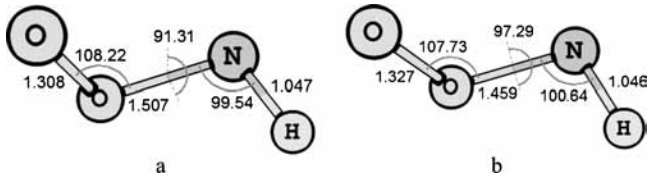

Figure 2. *cis*/*trans*-Conformations of TS for (a) singlet and (b) triplet nitroso oxide.

Compared to the singlet PES, the triplet transition states are somewhat "later" as it could be seen from the N−O (O−O) interatomic distances of 1.759 (1.262) Å for *cis*-HNOO and 1.743 (1.259) Å for *trans*-HNOO, respectively. It may be concluded that the triplet nitroso oxide will be formed preferably in the *trans* form owing to the lower activation barrier.

In the reaction of imidogene with oxygen the competitive formation of nitroso oxide is obviously in favor of ^{1}HNOO (Figure 3a). Nevertheless, under certain conditions (e.g., in high-temperature regime) the triplet channel may be of importance in the nitroso oxides chemistry.

HNOO Decomposition via O−O Bond Breaking. Taking into account the spin conservation rule one may assume that the O−O bond decomposition of singlet nitroso oxide should lead to atomic oxygen (^{3}P) and nitrosyl hydride in the triplet state (A″, $\pi\sigma$-biradical). Indeed, the relaxed scan showed the Morse-shaped curvature of the singlet PES led to these species (Figure 3b).

The study of the triplet PES of planar (*cis* and *trans*) nitroso oxides along the O−O bond reaction coordinate revealed the intersection of two electronic states for each HNOO conformation (Figure 3b). At r(OO) > 1.9 Å, the low-lying electronic state corresponds to $\sigma\sigma$-biradical with unpaired electrons located on the terminal oxygen (HNO(^{1}X) + O(^{3}P)). As could be seen from Figure 3b as well as the schematic orbital picture in Figure 4c this term is repulsive. Another state is best described as the $\pi-\pi$-triplet nitroso oxide (Figure 4a) and at long enough O−O distance as the HNO(^{3}A″, $\pi\sigma$-biradical) + O(^{3}P) pair (Figure 4b). The transition between these electronic states seems to be unlikely due to orbital symmetry or spin prohibition. Thus, the triplet nitroso oxide dissociation in the plane has to lead to the triplet nitrosyl hydride and atomic oxygen (^{3}P). However, attempts to locate the TS of this reaction resulted in a saddle point with two imaginary frequencies: the first one corresponds to the O−O bond cleavage and the second one to rotation around the N−O bond.

Reoptimization without symmetry restrictions allowed us to find the TS of *cis*-^{3}HNOO decomposition with D(HN−OO) = 39.7° and the only imaginary frequency, which corresponds to releasing the terminal O-atom (Figure 5a). A similar TS was found for the *trans*-^{3}HNOO, D(HN−OO) = 138.1°. Noteworthy, both TSs are "earlier" (e.g., R(O−O) = 1.625 Å for *gauche*-TS) than that concluded from the scanning diagram (1.76−1.80 Å, Figure 3b) presumably due to C_s symmetry restrictions during PES scanning.

We believe that out-of-plane distortion of the triplet nitroso oxide will allow direct decomposition of ^{3}HNOO into nitrosyl hydride in the ground state. Schematic representation of this possibility is depicted in Figure 4d. Following the internal reaction coordinate (Figure 5a) we found the N−O bond length to be reduced to 1.223 Å and the HNO valence angle approaches 109°. These geometric parameters are distinctly characteristic for the ground state of nitrosyl hydride (Table 3), thus justifying our conclusion.

Proton Transfer to the Terminal Oxygen Atom. According to ref 27, *cis*-HNOO can isomerize via proton transfer to the terminal oxygen atom. The authors localized a diamond-shaped TS (^{1}A′, E_a = 74 kJ·mol^{-1}) leading finally to NO + OH products. We also optimized this TS and proved its relation to reaction 13 by means of IRC (Figure 5b). According to our results, the activation energy was somewhat higher (112−121 kJ·mol^{-1} depending on the level of theory, Table 2); the thermal effect was found to be 103−123 kJ·mol^{-1}. Our attempts to locate the analogous TS on triplet PES were unsuccessful.

HNOO Isomerization to Dioxaziridine. It was suggested that nitroso oxide may isomerize to a three-membered cyclic peroxide, dioxaziridine, with the activation enthalpy lying between 170 and 190 kJ·mol^{-1}.[4,11],[27,38] According to our RI-MR-CISD(18;13)+Q/*aug*-cc-pVTZ calculations, this value was found to be 156.6 and 159.9 kJ·mol^{-1} for *cis*- and *trans*-nitroso oxide, respectively. The authenticity of localized saddle points to reactions 14 and 15 was confirmed by the IRC procedure (Figure 5c). Calculation of vertical singlet−triplet gaps shows the approach of PESs (Figure SI.2, Supporting Information) near the transition state; nevertheless, the intersection between these surfaces was not located.

4. Discussion

Relative Stability of HNOO Isomers. As above-mentioned, singlet nitroso oxides can exist in two isomeric forms, *cis* and

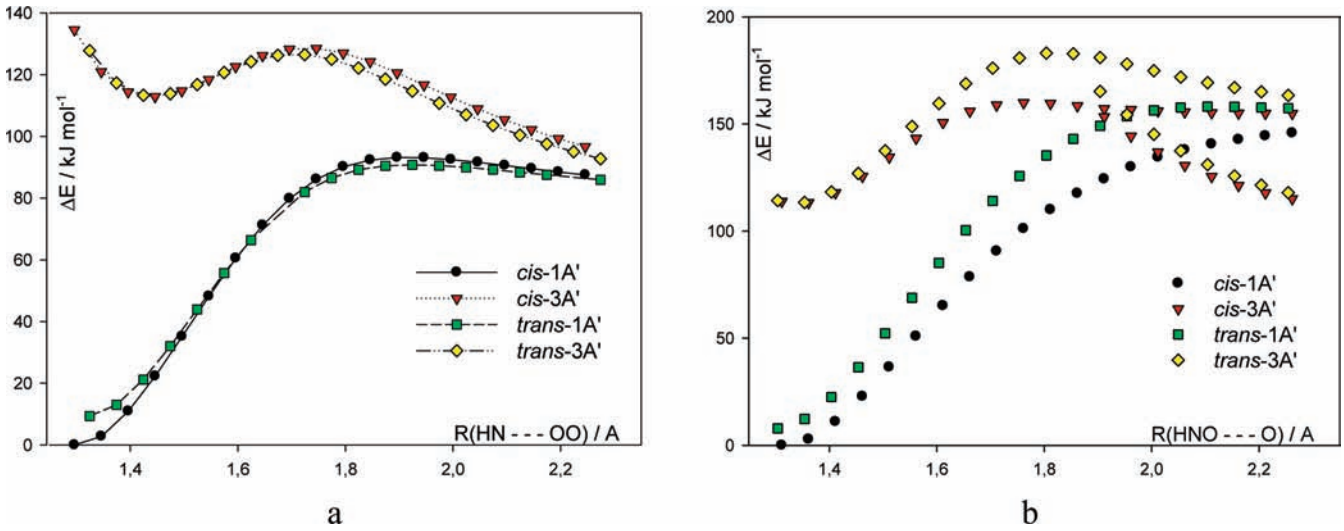

Figure 3. Relaxed scan of the HNOO PES on the (a) N−O and (b) O−O bond; MC-QDPT2(18;13)//CASSCF(18;13)/6-311+G(d,p).

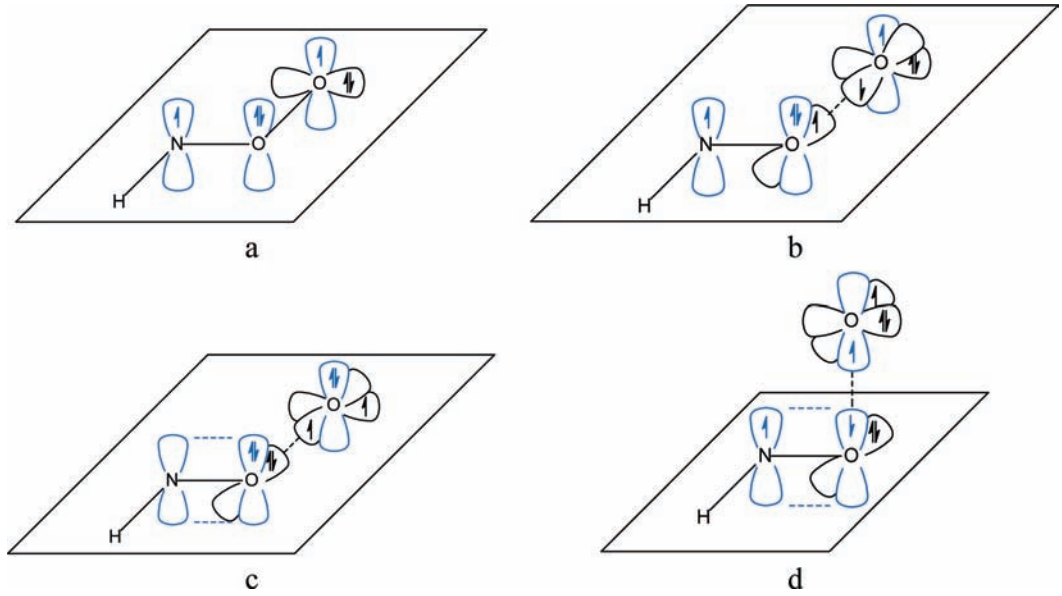

Figure 4. Schematic orbital picture of (a) 3A′ (π,π)-HNOO, (b) O-ejection TS, (π,π) 3A′, (c) repulsing term, (σ,σ) 3A′, and (d) O-abstraction TS with releasing from the plane, (π,π) 3A.

trans, which differ in the orientation of the terminal oxygen atom relative to the substituent at the nitrogen atom. At first glance the question of the relative stability of HNOO isomers is rather trivial. A lot of calculations ultimately predict that the *cis* form is more stable. The *cis*/*trans* energy gap depends on the level of theory being 18.0 kJ·mol^{-1} (CASSCF(6;6)/6-31G(d,p)[27]), 5.0 kJ·mol^{-1} (MP4(SDTQ)//MP2/6-31G(d,p)[43]), 7.5 kJ·mol^{-1} (MP2/6-31G(d,p)[44]), and 16.7 kJ·mol^{-1} (B3LYP/6-31G(d)[12]). To our knowledge, the only quantum chemical study performed at the MRD-CI//MCSCF(6;6)/6-31G(d,p) level of theory testifies to the higher stability of the *trans* form by 3.0 kJ·mol^{-1}.[27] However, FTIR investigation of HN_3 photooxidation[17] indicates formation of the only primary product, *trans*-HNOO, in the nitrene−dioxygen recombination. The authors also carried out a number of calculations at the RHF, DFT, and CCSD(T) levels of theory, which again predict the superior stability of the *cis* form by 12−21 kJ·mol^{-1}. To overcome this contradiction, Laursen et al.[17] gave three possible explanations, which may be reduced to the following. (1) Both *cis*- and *trans*-HNOO are formed initially, but rotational isomerization results in an equilibrium distribution of isomers. Taking into account the known inadequacy of the single-reference methods for the thermochemistry of ozone and isoelectronic species like HNOO, authors[17] adopted the Fueno's MRD-CI energy gap between HNOO isomers, which allows estimating a *trans*/*cis* ratio of over 1300:1 at 50 K. (2) A polarizable xenon matrix may solvate nitroso oxide, which is a member of the class of molecules known as 1,3-dipoles. The larger value of a dipole moment for *trans*-HNOO (2.6 vs 1.5 D, DFT calculations[17]) suggests preferential stabilization of the *trans*-isomer. (3) Lastly, Laursen et al. pointed out that "trapping of a single isomer may be result of reaction dynamics, for instance a small barrier (perhaps matrix-related) *or* a large barrier to rotational isomerisation".[17]

The former explanation is less acceptable to us. First, an interconversion of isomers should be of negligible importance due to a high activation barrier (Table 2, entry 1). Second, the explanation is based on the Fueno's result,[27] which is, in our opinion, rather questionable. As seen in Table 1, in ref 27 the calculated O−O interatomic distance in HNOO is too short and strongly differs from that of all other calculations. Our doubts are emphasized by the following arguments. (1) All theories

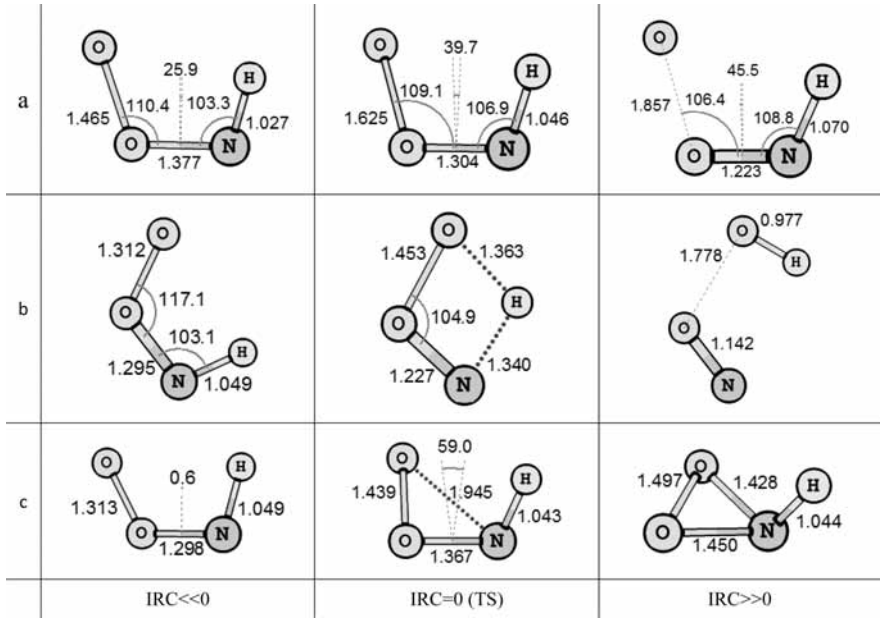

Figure 5. Structures of TS and the IRC scan for reactions 11 (a), 13 (b), and 14 (c); see Scheme 1.

TABLE 3: Geometric Parameters of Nitrosyl Hydride, CASSCF(12;9)/6-311+G(d,p)

HNO	*R*(HN), Å	*R*(NO), Å	*A*(HNO), deg
X (1A′)	1.079	1.212	109.0
1A″	1.040	1.238	118.1
3A″	1.057	1.266	110.8

(DFT, CC, CAS-SCF, MR-AQCC, see Table 1) give close results in reproducing the HNOO geometry with the O−O bond distance being 1.281−1.299 Å (*trans*-HNOO), whereas Fueno's calculations underestimate the peroxide bond length by 0.03−0.05 Å. In the case of *cis*-HNOO, the difference is even more pronounced. (2) The coupled clusters results obtained by DeKock et al.[16] (Table 1) fairly reproduce the vibrational nature of *trans*-HNOO, thus justifying the applicability of this method for nitroso oxide geometry calculations. (3) The computational method used by Fueno et al.[27] includes several simplifications: they used a rather small (6;6) active space with frozen low-lying molecular orbitals. We improved the computational scheme by (i) expanding the active space up to (18;13, i.e., all valence orbitals), (ii) unfreezing the remaining MOs, and (iii) enlarging the basis set to 6-311+G(d,p). We found that the O−O bond distance of HNOO is substantially elongated compared to that of Fueno and is in accordance with sophisticated MR-AQCC calculations (Table 1).

Thus, we recalculated the energies of the HNOO isomeric forms and found the higher stability of the *cis*-conformer. In order to obtain additional confirmation, we performed a number of composite computations (Table 2). The relative difference in *cis*/*trans* energies was found to be well reproduced by all the methods applied. Thus, we believe *cis*-HNOO is more stable, and therefore, the preferable formation of *trans*-nitroso oxide under the low-temperature conditions should not be explained by thermochemical reasons.

Analyzing another possibility of an extra-stabilization of *trans*-HNOO related to induced polarization of a xenon matrix by 1,3-dipole, one should keep in mind that, once formed, both isomers may interact with the matrix to a different extent, lowering the total energy of a system. However, because of the strictly hindered conformational isomerism of HNOO (see above), the *cis*/*trans* distribution will still be determined by the primary recombination reaction, NH + O_2. It clearly indicates that the clue to Laursen's experimental vs theoretical charade should be searching the peculiarity of the latter interaction.

For this purpose we localized both transition states to *cis*- and *trans*-HNOO at the CASSCF(18;13)/6-311+G(d,p) level of theory and evaluated the height of the activation barriers (Table 2). Indeed, we found the *trans*-PES around the saddle point lies under the corresponding one for the *cis* form by a few kJ·mol^{-1}. A more intensive account of the electron correlation as well as a basis set expanding trend decreases the activation energy to its disappearance; nevertheless, the *trans*-PES keeps lying below the *cis* one.

At present, our results do not give a definitive answer on the existence of the activation barrier for NH + O_2 recombination. In order to estimate competitive *cis*/*trans*-HNOO formation we used the variation method of the transition state theory. Accordingly, the reaction rate constant will correspond to the maximum of an activation free energy ΔG (s), s, the reaction coordinate, eq 16.

$$k(T,s) = \frac{k_B T}{h} e^{-\Delta G(T,s)/k_B T} \tag{16}$$

We assumed that ΔG_{max} corresponds to the found saddle point. Although this supposition is not evidently strict, it is reasonable for comparative estimation. At the MR-CISD(18;13)+Q/*aug*-cc-pVTZ//CAS-SCF(18;13)/6-311+G(d,p) level of theory $\Delta G^{\ddagger}$(eq 3) = 31.1 kJ·mol^{-1} and $\Delta G^{\ddagger}$(eq 4) = 28.8 kJ·mol^{-1}. The observed difference in $\Delta G^{\ddagger}$ is quite enough to ensure the less stable isomer will be undetectable at 50 K (a lower limit for the energy difference of 2 kJ·mol^{-1} was estimated by the authors of ref 17). Moreover, our calculations yield a dipole moment larger for the *trans* saddle point (1.6 D) than for the *cis* one (1.2 D), suggesting that xenon should additionally stabilize the *trans* TS and increase $\Delta\Delta G^{\ddagger}$. Thus, the ratio of the rate constants of reactions 3 and 4 at 50 K is less or, at least, equal to 7.3 × 10^{-4}, explaning the exclusive formation of *trans*-HNOO despite the superior stability of the *cis*-nitroso oxide. In fact, the latter explanation of the experimental results given by Laursen et al.[17] is almost in line with our theoretical calculations, if conjunction "or" (see citation above) is replaced by "and".

Our results allow concluding that increasing temperature will (i) equalize the *cis*/*trans*-HNOO formation rate constants and (ii) accelerate conformational interconversion between these forms. Both factors cause growth of *cis*-HNOO content, and under high enough temperature conditions, the ratio of the nitroso oxide isomers should obey to the Boltzmann distribution (ca. *cis:trans* = 7:1 at 600 K, 1.8:1 at 2000 K). It means that the moderate- and high-temperature chemistry of nitroso oxide should be the subject for both isomers transformation.

Kinetic Model. The RRKM theory was used for the calculation of microscopic rate constants $\kappa_1-\kappa_{15}$ for all reactions presented in Scheme 1. This theory presupposes use of energies, ZPEs, and frequencies, which were obtained by ab initio calculation. As above-mentioned an intensive account of electron correlation is essential to provide reliable results. It predetermines appliance of the multireference MC-QDPT2, MRCI, and MR-AQCC methods. For reasonable estimation of reaction energies we also used G3, G3MP2B3, CBS-QB3, and W1U procedures. However, in the latter computational schemes structure optimization is performed using density functional theory, which is known to insufficiently account for the static contribution to the correlation energy.[15,45] Actually, we found that DFT calculations cannot correctly reproduce the most problematic parts of the HNOO PES. It limits the applicability of the composite methods to RRKM calculations, so we used them for comparative purposes. In common, there is a good consistency in the energy calculations by composite and multireference methods for all minima and several saddle points on the PES. This result indicates the static electronic correlation to be less important for these stationary points as well as full enough account of dynamic correlation energy by multireference methods. From the row of these methods, the most sophisticated level of theory (RI-MR-CISD(18;13)+Q/*aug*-cc-pVTZ) was chosen for kinetic analysis, since it gives the closest results to composite procedures.

The apparent rate constants k_1-k_8 were calculated according to eqs 2 and 3 for the 214−2500 K temperature range. The tunneling effect of proton transfer (reaction 13), which is important for the rate constant k_1, was estimated by eq 6. The total rate constant k_{total} for the NH + O_2 reaction was calculated as a sum of the apparent k_1-k_8 rate constants. The values of the reaction rate constants are given in Table SI.1, Supporting Information; the results of their approximation in terms of the three-parameter Arrhenius equation in eq 1 are listed in Table SI.2, Supporting Information. The experimental data obtained in a number of works[18,20,21,24,25,46] for the overall 293−3270 K diapason are in satisfactory agreement with k_{total}. As seen in Figure 6, the temperature dependence of k_{total} is rather nontrivial and consists of three quasi-linear intervals.

Low-Temperature Chemistry. The first of them corresponds to low-temperature diapason (up to room temperature). Under these conditions all ways for the transformation of "hot" nitroso oxide particles are of negligible importance and the thermal deactivation and accumulation of HNOO becomes the dominant process channel. Production of HNOO falls off with increasing temperature, as typically observed for radical addition reactions without low-energy exit channels, thus explaining the slightly negative activation energy of −3.4 kJ·mol^{-1} for k_{total}. The low-temperature chemistry of HNOO obviously includes other possibilities of nitroso oxide transformations which are beyond the scope of our work, namely, bimolecular decay of HNOO, photoreactions, or O-atom transfer to appropriate substrate. These processes are known to be important in the condensed phase chemistry of aromatic nitroso oxides.[3–10,47]

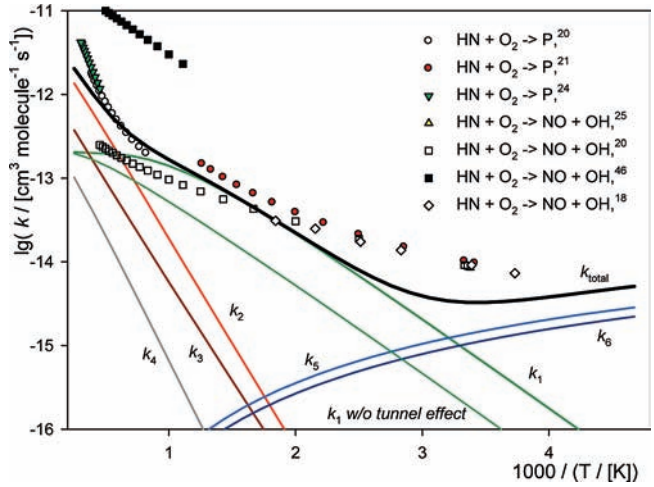

Figure 6. Temperature dependence of the apparent rate constants k_1-k_6 as well as of the overall k_{total} for the NH + O_2 reaction.

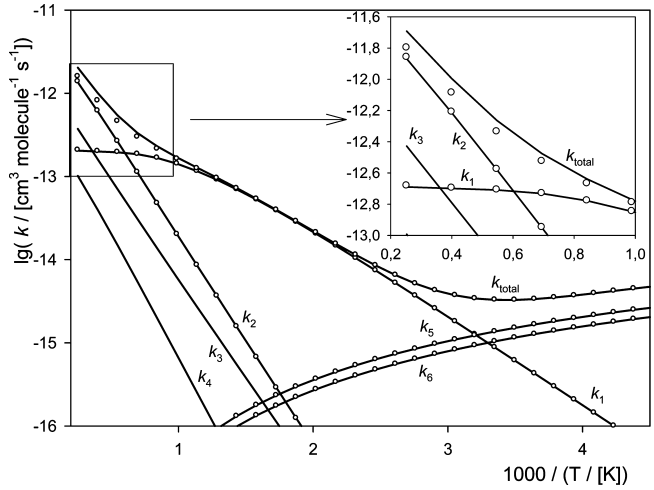

Figure 7. Comparison of the full (solid lines) and reduced (circles) kinetic schemes for the NH + O_2 reaction.

SCHEME 2

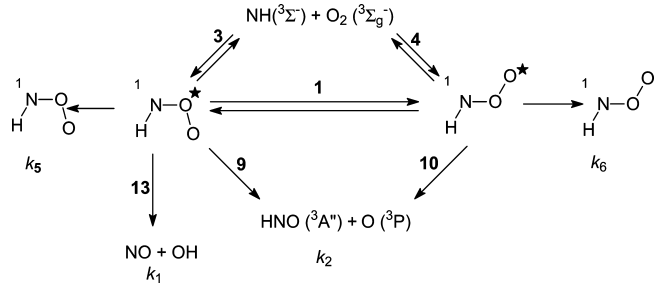

Medium-Temperature Chemistry. When temperature increases above 400 K the reaction system turns into a qualitatively different state. Formation of the NO + OH radical pair becomes the dominant process as it was shown in a number of experimental works.[20,46] There is a fine agreement between our results and available kinetic data (Figure 6). The adequate description of the NO + OH formation kinetics was achieved only by the tunnel effect. The probability of proton tunneling in reaction 13 was found to be as large as 4.2 at a temperature of 214 K and was decreased to 1.2 at 2500 K.

Since in the gas-phase kinetics at ambient temperatures NO + OH formation is the rate-determining channel, the mechanism of this reaction was the primary objective in a number of investigations. Thus, Melius and Miller[28] suggested the mech-

anism of products formation (Figure 1a) as a row of consecutive transformations: through HNOO (recombination), dioxaziridine (cyclization), hydrogen nitryl (O−O bond cleavage), nitrous acid (isomerization), and finally NO + OH radical pair (dissociation). However, as seen in Figure 6 and Table SI.1, Supporting Information, the rate constant of ring closure k_4 is too small to effect on the overall reaction kinetics due to the high activation energy (Table SI.2, Supporting Information). On the basis of the same argumentation, Fueno concluded[27] that HNOO isomerizes into hydroperoxynitrene:NOOH (Figure 1b) through the activation barrier of 74 kJ·mol^{-1} rather than forming a three-membered cycle with an activation energy of 189 kJ·mol^{-1}. Further, hydroperoxynitrene easily dissociates into nitrogen mono-oxide and hydroxyl radical.

Our results unambiguously confirm Fueno's mechanism despite the considerable difference in the activation barrier and heat of reaction in eq 13, as well as in the optimized geometry of HNOO (see above), the transition state, and hydroperoxynitrene. We found that both composite (112.5−116.1 kJ·mol^{-1}) and multireference (118.4−120.8 kJ·mol^{-1}) methods fairly reproduce the height of the H-atom transfer activation barrier, thus justifying our estimation of the reaction energetics. As above-mentioned, the MCSCF and MRCI computational procedures applied by Fueno suffer from a number of shortcomings. In our opinion, the main one is a rather small (6;6) active space which poorly reproduces the geometrical parameters and seems to allow only a qualitative description of the PES shape.

The hydroperoxynitrene structure is the distinctive example of this conclusion. Indeed, according to Fueno,[27] this intermediate may be represented as nitrene with an O−O bond length of 1.472 Å, which is typical for peroxy compounds (e.g., 1.452 for hydrogen peroxide[48]). In this connection, Fueno's supposition of covalent peroxide bond dissociation with a low activation energy seems to be doubtful. We carefully investigated the geometry of hydroperoxynitrene with various methods and found out that different model chemistries give a highly elongated O−O bond: 1.866, 1.971, and 2.030 Å for CCSD, MP4(SDQ), and MR-AQCC(10;8) with the 6-311+G(d,p) basis set, respectively. The results obtained by a number of density functionals are consistent with that of ab initio methods (e.g., 1.913 Å for mPWB95/6-311+G(3df,2p)). The long-range O−O bond indicates that the NOOH particle is rather a complex of two radicals than the covalent-bonded molecule. The electronic structure of NOOH is nontrivial and currently under investigation in our laboratory.

Thus, the agreement of theoretical and experimental results proves that the medium-temperature chemistry of the NH + O_2 reaction proceeds via isomerization of *cis*-HNOO through a diamond-shaped TS (Figure 5b) to a weakly bonded NOOH intermediate which is easily decomposed to the ultimate products, the NO + OH radical pair. The effective activation energy of k_{total} for the medium-temperature interval was found to be 17.0 kJ·mol^{-1}.

High-Temperature Chemistry. At temperatures of ∼1000 K decomposition of HNOO into nitrosyl hydride and atomic oxygen (reactions 9−12, Scheme 1) becomes competitive with H-atom transferring (reaction 13). When temperature increases, the Arrhenius slope of k_{total} is mainly determined by the O−O dissociation reaction. This result is in agreement with generally accepted conclusion that the nitrosyl hydride is the main product of the high-temperature channel,[19,24,27,28] although, to the best of our knowledge, there is no kinetic study of the NH + O_2 system based on direct monitoring of the HNO concentration.

It is noteworthy that both Fueno[27] and Melius[28] assumed the formation of atomic oxygen and nitrosyl hydride to proceed via the *triplet* form of HNOO. Although our finding does not rule out this possibility, the main source of the HNO was found to be the *singlet* nitroso oxide. Indeed, the kinetic analysis of Scheme 1 shows linearity of the logarithm of k_2 and k_3 vs $1/T$ in a wide temperature interval and prevailing of *singlet* HNOO decomposition over the *triplet* one with a factor of 3.3−3.8 (1000−2500 K). Thus, the temperature dependence of k_{total} is determined by that of k_2 and k_3, giving an effective activation energy of 37.2 kJ·mol^{-1} ($T > 1400$ K).

Obviously, in the O−O decomposition reaction the electronic nature of the product (HNO) depends on that of the reactant (HNOO), as analyzed in the Results section.

Taking into account that another decomposition product, atomic oxygen, is ultimately formed in the ^{3}P state (because the ^{1}D state lies 189.8 kJ·mol^{-1} higher), the *singlet* HNOO produces the *triplet* nitrosyl hydride and vice versa. According to the kinetic analysis, a considerable amount of HNO is formed in the ^{3}A″ state. Unfortunately, the strongly forbidden nature of the transition between the singlet and triplet manifolds has prevented direct observation of the triplet state using optical techniques.[49] One may only suppose that, depending on the reaction system composition and experimental conditions, ^{3}HNO underwent either physical quenching or chemical transformation. In particular, possible HNO reactions in rich ammonia flames were discussed by Dean.[50]

Conclusions

A detailed study of the reaction of triplet nitrene HN with dioxygen has been performed using a variety of computational procedures and RRKM theory. The potential energy surface of the NH + O_2 reaction has been carefully investigated by means of sophisticated multireference MC-QDPT2, MRCI, and MR-AQCC calculations as well as G3, G3MP2B3, CBS-QB3, and W1U composite methods. The complete set of stationary points has been localized. The reaction occurs via intermediate formation of hot nitroso oxide HNOO, which further undergoes either dissipation of excess energy (low-temperature reaction channel) or dissociation of the N−O (back to the reactants), O−O (HNO + O formation, high-temperature channel), and H−N bonds (accompanied by proton transfer to the terminal O atom, thus leading to the NO + OH radical pair, medium-temperature channel). Isomerization of HNOO into dioxaziridine, which was adopted in a number of papers[19,28,38] as a possible route of NO + OH formation, does not compete with the latter reaction due to the high activation energy and, consequently, low rate constant.

In accordance with a number of previous investigations,[12,27,43,44] we demonstrated the coexistence of the *cis* and *trans* forms of hydrogen nitrosyl oxide with the preponderance of *cis*-HNOO, the *cis*/*trans* energy gap was found to be 8.1−10.9 kJ·mol^{-1}. Contrary to thermodynamics, formation of the *trans* form of HNOO is favorable as it follows from the PES curvature for both conformers (Figure 3). The ratio of rate constants of *cis*/*trans*-nitroso oxide formation is 7.3×10^{-4} at 50 K, thus explaining Laursen's FTIR observation of superior formation of *trans*-HNOO.[17] Under medium- and high-temperature conditions, the ratio of the nitroso oxide isomers obeys the Boltzmann distribution (ca. *cis*:*trans* = 7:1 at 600 K, 1.8:1 at 2000 K). Thus, both isomers play an important role in the HN + O_2 reaction.

Although all employed levels of theory give consistent results on the NH + O_2 reaction energetics, we cannot localize the transition states of the reactions 1 and 3−10 using composite

methods. The most possible reason is a poor description of the multireference nature of the open shell singlets by the DFT procedures used in composite calculations for geometry optimization. Thus, an intensive account of both static and dynamic contributions to the electron correlation energy is essential to provide a reliable estimation of molecular geometries and energies.

The energies of the reactants, products, and transition states were calculated at the RI-MR-CISD(18;13)+Q/*aug*-cc-pVTZ level of theory; vibrational analysis of these species was done by means of CASSCF(18;13)/6-311+G(d,p). The obtained data were used for the RRKM kinetic analysis of the Scheme 1. The main results of the analysis are (1) the calculated total rate constant corresponds to available experimental data both qualitatively (fairly reproducing the high-temperature curvature of $\log(k_{total})$ vs $1/T$, Figure 6) and quantitatively, (2) the low-temperature chemistry of the HN + O_2 interaction is accompanied with a negative activation energy due to prevailing stabilization, not transformation of HNOO, and (3) the set of apparent rate constants allows comparing the rates of competitive reactions and thus reducing the reaction mechanism. The more motivated simplification is related to neglecting dioxaziridine formation and, hence, its further transformations. A somewhat less strict simplification that may be applied is elimination of triplet HNOO reactions from the reaction mechanism. Indeed, the reduced model of the reaction mechanism depicted in Scheme 2 gives almost the same values of the apparent rate constants and the resulting k_{total} and the same curvature of $\log(k_{total})$ vs $1/T$ in the whole temperature interval (Figure 7) as the full mechanism (Scheme 1) does. The only distinctive difference between both mechanisms may be observed at $T > 1000$ K (Figure 7, top-right corner).

Thus, we may conclude that our approach (MRCI + RRKM) allows precisely describing the process involving a number of reactions of parent nitroso oxide, HNOO. We believe that our work gives deeper insight into the nature of the nitroso oxide moiety and provides a basis for further investigation of substituted nitroso oxides chemistry. At present, study of the aromatic nitroso oxides reactivity is in progress in our laboratory.

Acknowledgment. This work was funded by the program of the RAS "Theoretical and experimental study of the nature of chemical bonding and mechanisms of most important chemical reactions and processes".

Supporting Information Available: Detailed formulas for calculation of the appropriate rate constants, figures related to the conformational potential of ^{3}HNOO, IRC scan for reaction 15, *X*,*Y*,*Z* coordinates of all stationary points, and values of apparent rate constants with their approximation in terms of a three-parameter Arrhenius equation. This material is available free of charge via the Internet at http://pubs.acs.org.

References and Notes

(1) Brinen, J. S.; Singh, B. *J. Am. Chem. Soc.* **1971**, *93*, 6623.
(2) Singh, B.; Brinen, J. S. *J. Am. Chem. Soc.* **1971**, *93*, 540.
(3) Gritsan, N. P. *Russ. Chem. Rev.* **2007**, *76*, 1139.
(4) Sawwan, N.; Greer, A. *Chem. Rev.* **2007**, *107*, 3247.
(5) Chainikova, E.; Khursan, S.; Safiullin, R. *Kinet. Catal.* **2006**, *47*, 549.
(6) Chainikova, E. M.; Khursan, S. L.; Safiullin, R. L. *Dokl. Phys. Chem.* **2005**, *403*, 133.
(7) Safiullin, R.; Khursan, S.; Chainikova, E.; Danilov, V. *Kinet. Catal.* **2004**, *45*, 640.
(8) Chainikova, E. M.; Khursan, S. L.; Safiullin, R. L. *Kinet. Catal.* **2004**, *45*, 794.
(9) Chainikova, E. M.; Khursan, S. L.; Safiullin, R. L. *Dokl. Phys. Chem.* **2004**, *396*, 138.
(10) Chainikova, E. M.; Khursan, S. L.; Safiullin, R. L. *Dokl. Phys. Chem.* **2003**, *390*, 163.
(11) Zelentsov, S. V.; Zelentsova, N. V.; Shchepalov, A. A. *High Energy Chem.* **2002**, *36*, 326.
(12) Zelentsov, S. V.; Zelentsova, N. V. Nitroso Oxides: Their Properties and Role in Photochemistry. In *Peroxides at the Beginning of the Third Millenium*; Antonovsky, V. L., Ed.; Nova Science Publishers, Inc.: New York, 2004; Vol. 12; p 239.
(13) Talipov, M. R.; Khursan, S. L.; Safiullin, R. L. *Bashkirskiy Khim. J.* **2006**, 105.
(14) Zelentsov, S. V.; Shchepalov, A. A. *Vestnik Nizhegorodskogo Univ., Ser. Khim.* **2001**, 120.
(15) Jensen, F. *Introduction to Computational Chemistry*; John Wiley & Sons: New York, 1999.
(16) DeKock, R. L.; McGuire, M. J.; Piecuch, P.; Allen, W. D.; Shaefer, H. F., III; Kowalski, K.; Kucharski, S. A.; Musial, M.; Bonner, A. R.; Spronk, S. A.; Lawson, D. B.; Laursen, S. L. *J. Phys. Chem. A* **2004**, *108*, 2893.
(17) Laursen, S. L.; Grace, J. E., Jr.; DeKock, R. L.; Spronk, S. A. *J. Am. Chem. Soc.* **1998**, *120*, 12583.
(18) Hack, W.; Kurzke, H.; Wagner, H. G. *J. Chem. Soc., Faraday Trans.* **1985**, *2*, 949.
(19) Dean, A. M.; Bozzelli, J. W. Combustion Chemistry of Nitrogen. In *Gas-Phase Combustion Chemistry*; Gardiner, W. C., Jr., Ed.; Springer: New York, 2000; p 125.
(20) Romming, H. J.; Wagner, H. G. *Symp. Int. Combust. Proc.* **1996**, *26*, 559.
(21) Lillich, H.; Schuck, A.; Volpp, H.-R.; Wolfrum, J. *Symp. Int. Combust. Proc.* **1994**, *25*, 993.
(22) Baulch, D. L.; Cobos, C. J.; Cox, R. A.; Frank, P.; Hayman, G.; Just, T.; Kerr, J. A.; Murrells, T.; Pilling, M. J.; Troe, J.; Walker, R. W.; Warnatz, J. *J. Phys. Chem. Ref. Data* **1994**, *23*, 847.
(23) Baulch, D. L.; Cobos, C. J.; Cox, R. A.; Esser, C.; Frank, P.; Just, T.; Kerr, J. A.; Pilling, M. J.; Troe, J.; Walker, R. W.; Warnatz, J. *J. Phys. Chem. Ref. Data* **1992**, *21*, 411.
(24) Mertens, J. D.; Chang, A. Y.; Hanson, R. K.; Bowman, C. T. *Int. J. Chem. Kin.* **1991**, *23*, 173.
(25) Zetzsch, C.; Hansen, I. *Ber. Bunsen-Ges. Phys. Chem.* **1978**, *82*, 830.
(26) NIST Chemical Kinetics Database on the Web, Standard Reference Database 17.
(27) Fueno, T.; Yokoyama, K.; Takane, S. *Theor. Chim. Acta* **1992**, *82*, 299.
(28) Miller, J. A.; Melius, C. F. *Symp. Int. Combust. Proc.* **1992**, *24*, 719.
(29) Talipov, M.; Ryzhkov, A.; Hursan, S.; Safiullin, R. *J. Struct. Chem.* **2006**, *47*, 1051.
(30) Curtiss, L. A.; Raghavachari, K.; Redfern, P. C.; Rassolov, V.; Pople, J. A. *J. Chem. Phys.* **1998**, *109*, 7764.
(31) Curtiss, L. A.; Redfern, P. C.; Raghavachari, K.; Rassolov, V.; Pople, J. A. *J. Chem. Phys.* **1999**, *110*, 4703.
(32) Montgomery, J. J. A.; Frisch, M. J.; Ochterski, J. W.; Petersson, G. A. *J. Chem. Phys.* **1999**, *110*, 2822.
(33) Martin, J. M. L.; de Oliveira, G. *J. Chem. Phys.* **1999**, *111*, 1843.
(34) Granovsky, A. A. http://classic.chem.msu.su/gran/gamess/index.htm.
(35) Schmidt, M. W.; Baldridge, K. K.; Boatz, J. A.; Elbert, S. T.; Gordon, M. S.; Jensen, J. H.; Koseki, S.; Matsunada, N.; Nguyen, K. A.; Su, S. J.; Windus, T. L.; Dupuis, M.; Montgomery, J. A. *J. Comput. Chem.* **1993**, *14*, 1347.
(36) Neese, F. *J. Chem. Phys.* **2003**, *119*, 9428.
(37) Dean, A. M. *J. Phys. Chem.* **1985**, *89*, 4600.
(38) Nguyen, M. T.; Sumathi, R.; Sengupta, D.; Peeters, J. *Chem. Phys.* **1998**, *230*, 1.
(39) Robinson, P. J.; Holbrook, K. A. *Unimolecular Reactions*; Wiley-Interscience: New York, 1972.
(40) Troe, J. *J. Chem. Phys.* **1977**, *66*, 4758.
(41) Miller, W. H. *J. Am. Chem. Soc.* **1979**, *101*, 6810.
(42) Hammond, G. S. *J. Am. Chem. Soc.* **1955**, *77*, 334.
(43) Li, Y.; Iwata, S. *Bull. Chem. Soc. Jpn.* **1997**, *70*, 79.
(44) Nakamura, S.; Takahashi, M.; Okazaki, R.; Morokuma, K. *J. Am. Chem. Soc.* **1987**, *109*, 4142.
(45) Cramer, C. J. *Essentials of Computational Chemistry*, 2nd ed.; John Wiley & Sons: Chichester, 2004.
(46) Bian, J.; Vandooren, J.; Van Tiggelen, P. J. *Symp. Int. Combust. Proc.* **1991**, *23*, 379.
(47) Ishikawa, S.; Tsuji, S.; Sawaki, Y. *J. Am. Chem. Soc.* **1991**, *113*, 4282.
(48) Koput, J. *Chem. Phys. Lett.* **1995**, *236*, 516.
(49) Ellis, J. H. B.; Ellison, G. B. *J. Chem. Phys.* **1983**, *78*, 6541.
(50) Dean, A. M.; Chou, M.-S.; Stern, D. *Int. J. Chem. Kinet.* **1984**, *16*, 633.

JP902527A